International Journal of Remote Sensing
Vol. 27, No. 7, 10 April 2006, 1453–1464

Taylor & Francis
Taylor & Francis Group

Spectral or spatial quality for fused satellite imagery? A trade-off solution using the wavelet *à trous* algorithm

MARIO LILLO-SAAVEDRA*† and CONSUELO GONZALO‡
†Faculty of Agricultural Engineering, University of Concepción, Chile
‡Computer School, Department of Architecture and Technology of the Computer, Technical University of Madrid, Spain

(*Received 3 September 2004; in final form 7 November 2005*)

Several different methods for the fusion of multispectral and panchromatic images based on the wavelet transform have been proposed. The majority provide satisfactory results, but there is one, the *à trous* algorithm, that presents several advantages over the other fusion methods. Its computation is very simple; it only involves elementary algebraic operations, such as products, differences and convolutions. It yields a better spatial and spectral quality than the other methods. Standard fusion methods do not allow control of the spatial and spectral quality of the fused image; high spectral quality implies low spatial quality and vice versa. This paper proposes a new version of a fusion method based on the wavelet transform, computed through the *à trous* algorithm, that permits customization of the trade-off between the spectral and spatial quality of the fused image through the evaluation of two quality indices: a spectral index (the ERGAS index) and a spatial one. For the latter, a new spatial index based on ERGAS concepts and translated to the spatial domain has been defined. In addition, several different schemes for the computation of the fusion method investigated have been evaluated to optimize the degradation level of the source image required to perform the fusion process. The performance of the proposed fusion method has been compared with the fusion methods based on wavelet Mallat and filtering in the Fourier domain.

1. Introduction

Among the strategies for the fusion of multiresolution satellite images, the pyramidal algorithm of Mallat (Pohl and van Genderen 1998, Zhou *et al.* 1998, Mallat 1999, Pohl 1999, Ranchin and Wald 2000) is one of the most widely because of the high spectral quality of the resulting image, although its anisotropic nature still produces problems for the fusion of images with a large number of borders that are not horizontal, vertical or diagonal (Candès and Donoho 2000).

Dutilleux (1987) proposed a wavelet *à trous* ('with holes') algorithm that differs from the pyramidal ones in that it is a redundant, which implies that between two consecutive degradation levels there is no dyadic spatial compression of the original image, but rather the size of the image is maintained (figure 1). In addition, this algorithm is of an isotropic nature; that is, the basis of the pyramid represents the original image (figure 1(*a*)), and each of its levels is a degraded and compressed version of the image represented at the previous level. In this way, the spatial

*Corresponding author. Email: malillo@udec.cl

International Journal of Remote Sensing
ISSN 0143-1161 print/ISSN 1366-5901 online
http://www.tandf.co.uk/journals
DOI: 10.1080/01431160500462188

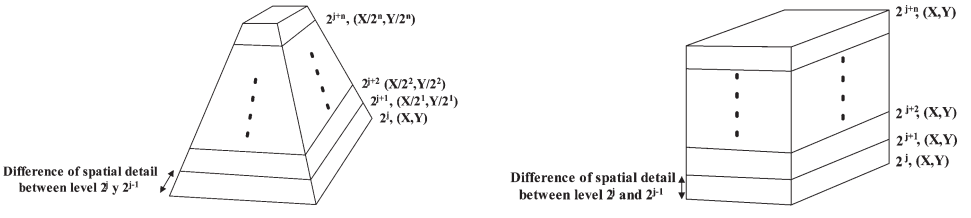

Figure 1. Degradation scheme for: (*a*) the Mallat algorithm, (*b*) the *à trous* algorithm.

resolution and the image size decrease from one level to the next. However, in figure 1(*b*), the spatial resolution decreases from a level to the next, but the image size is constant for all levels.

Comparative studies (Chibani and Houacine 2003, González-Audicana *et al.* 2005) have shown that both the spatial and the spectral quality of the fused images obtained by the *à trous* algorithm is better than that provided by the Mallat algorithm. Although for both fusion methods a wide range of strategies exists to integrate the spatial information contained in a panchromatic image (PAN), none of these strategies permits an objective control of the trade-off between spectral and spatial quality of the fused images. To mitigate this limitation, this work presents a new approximation of image fusion through the wavelet *à trous* algorithm that objectively establishes the degree of trade-off between spectral and spatial quality of the resulting image through curve characteristics (Gonzalo and Lillo 2004). These curves represent spatial and spectral quality indexes together, obtaining fused images adapted to user requirements.

As an index of the spectral quality of the fused image, the ERGAS (*Erreur Relative Globale Adimensionalle de Synthèse*) index (Wald 2000) was selected for its extensive use. It is defined and discussed in section 3. An index is also introduced to evaluate the spatial quality image: the spatial ERGAS index (Lillo-Saavedra *et al.* 2005). In both cases, the lower the ERGAS value, the better the quality of the fused image (Wald 2000). In this way, two indexes measuring quality with a different character that varies inside a similar range were used, making their representation in a common domain easier.

2. Fusion by the standard *à trous* algorithm

This algorithm consists basically in the application of consecutive convolutions between the image under analysis and a scaling function at distinct degradation levels (Garzelli *et al.* 2004, Gonzalo and Lillo 2004, González-Audicana *et al.* 2005). One of the most widely used scaling functions for the computation of the *à trous* algorithm is the b_3-spline (Núñez *et al.* 1999).

If the original image without degradation is represented by $I_j(x,y)$, the wavelet coefficients, $C_{j+n}(x,y)$, for the level $j+n$ are obtained by the difference between the corresponding two consecutive degraded images, $I_{j+n-1}(x,y)$ and $I_{j+n}(x,y)$, as shown in equation (1):

$$C_{j+n}(x, y) = I_{j+n-1}(x, y) - I_{j+n}(x, y) \tag{1}$$

To carry out an image synthesis from a degradation level $j+n$, an additive criterion should be applied in which all the coefficients obtained are added to the last

degradation level of the original image (equation (2)):

$$I_j(x, y) = I_{j+n}(x, y) + \sum_{k=1}^{n} C_{j+k}(x, y) \tag{2}$$

If $I_{j+n}(x,y)$ represents the successive degraded planes that contain the low frequency information of the original image, and $C_{j+n}(x,y)$ its respective wavelet coefficients, which contain the high frequency information, then it is possible to plant an image fusion scheme in which the low frequency information contained in a multispectral image (MULTI) with the high frequency information contained in the wavelet coefficients of a high resolution spatial image (PAN), to obtain a multispectral image of high spatial resolution.

Núñez *et al.* (1999) proposed two methodologies to fuse multispectral images with panchromatic images: the substitutive and the additive. In both methods, the MULTI image is resampled as the same size of the PAN image. The first of these methodologies consists in degrading in n wavelet planes the MULTI image through the *à trous* algorithm, separating in this way its low and high frequency content. In the same way, the PAN is decomposed. Finally, a fused image is obtained, substituting in the inverse transform the coefficients $C_{j+k}(x,y)$ of each band of the multispectral image for the sum of all the wavelet coefficients of the PAN image. The second methodology is additive, and degrades only the PAN image and integrates the sum of its wavelet coefficients to the different bands of the original MULTI image in a transformed inverse.

Both fusion strategies present two common problems. The first is the impossibility of controlling the trade-off inherent between the spectral–spatial quality of the fused image and the second is that information is integrated directly from the PAN image in the multispectral image, without considering the particular characteristics of each spectral band of the MULTI image. In this regard, some authors proposed the joint use of an Intensity Hue and Saturation (IHS) transform and a wavelet à trous algorithm for the fusion images (Chibani and Houacine 2002, González-Audicana *et al.* 2004). This fusion image method is based on a combination of IHS transform and redundant wavelet decomposition. The main idea consists of transforming multispectral images into independent IHS components. The intensity component is fused with a panchromatic image in the redundant wavelet domain through an appropriate model (Chibani and Houacine 2002).

To solve these problems, this paper proposes some modifications to the fusion criterion based on the *à trous* algorithm. Basically, they consist of establishing a mechanism that permits control of the spatial–spectral quality trade-off through the introduction of a weighting factor for the wavelet coefficients of the PAN image.

3. Quality measure of the fused image

The spectral quality of the fused images has been evaluated through the ERGAS index (Wald 2000) defined by equation (3):

$$\mathrm{ERGAS} = 100\frac{h}{l}\sqrt{\frac{1}{N_{\mathrm{Bands}}}\sum_{i=1}^{N_{\mathrm{Bands}}}\left(\frac{\mathrm{RMSE}^2(\mathrm{Band}_i)}{\mathrm{MULTI}_i^2}\right)} \tag{3}$$

where h and l represent the spatial resolution of the PAN and MULTI images, respectively, N_{Bands} is the number of bands of the fused image, $\mathrm{MULTI}_{\mathrm{i}}$ is the

radiance value of the ith band of the MULTI image and RMSE is defined as:

$$\mathrm{RMSE}(\mathrm{Band}_i) = \frac{1}{\mathrm{NP}} \sqrt{\sum_{k=1}^{\mathrm{NP}} (\mathrm{MULTI}_i(k) - \mathrm{FUS}_i(k))^2} \tag{4}$$

where NP is the number of pixels of the fused image and FUS_i represents the ith band of the fused image.

Given that in the definition of the ERGAS index (equation (3)), only spectral characteristics of the source images to be fused were considered, Lillo-Saavedra *et al.* (2005) proposed a new index with the objective of evaluating the spatial quality of these images. This new index is inspired by the spectral ERGAS and has been named spatial ERGAS. In its definition, a spatial RMSE has been included, which is defined as:

$$\mathrm{RMSE}(\mathrm{Band}_i) = \frac{1}{\mathrm{NP}} \sqrt{\sum_{k=1}^{\mathrm{NP}} (\mathrm{PAN}_i(k) - \mathrm{FUS}_i(k))^2} \tag{5}$$

where PAN_i is the image obtained by adjusting the histogram of the original PAN image to the histogram of the ith band of the MULTI image. And finally, MULTI_i must be replaced by PAN_i in equation (3).

4. Weighted fusion method by the *à trous* algorithm

The method of weighted fusion (Gonzalo and Lillo 2004) that this paper proposes is based on the substitutive fusion method of the *à trous* algorithm (Núñez *et al.* 1999). The modifications introduced in this fusion method, with the objective of eliminating the above-mentioned problems, consists basically of establishing a mechanism that permits control of the spatial–spectral quality trade-off through the introduction of a weighting factor of the wavelet coefficients from the PAN image. Equation (6) represents formally the algorithm of the proposed fusion:

$$\mathrm{FUS}_i(x, y) = I^i_{\mathrm{MULTI}_j}(x, y) + \alpha^i \sum_{k=1}^{W} C^i_{\mathrm{PAN}_k}(x, y) \tag{6}$$

where the indexes i and j represent the number of bands and the degradation level of the MULTI image, respectively. W corresponds to the number of wavelet planes to integrate from the PAN image to the MULTI image. It should be noted that for $\alpha = 100\%$, equation (6) represents the substitutive method of the *à trous* algorithm. The previous determination of the weighting factor of the wavelet coefficients of the PAN image, α^i, is performed by the simultaneous evaluation of the spectral and spatial quality of the fused images using the ERGAS indexes defined earlier for a range of values for α^i, which varies between 0% and 200%. This range can be grouped into three sets: (i) $0\% < \alpha^i < 100\%$, the wavelet coefficients of the PAN image are attenuated by the scalar α^i; and in this case the spectral quality of the fused image is improved. (ii) $\alpha^i = 100\%$, the wavelet coefficients of the PAN image are completely integrated; this case corresponds to the standard substitution method when using *à trous* algorithm. (iii) $100\% < \alpha^i < 200\%$, the wavelet coefficients of PAN image are amplified by the scalar α^i; in this case the spatial quality of the fused image is improved but its spectral quality is poorer.

As the best trade-off between the spectral and spatial quality of the fused image would be obtained when its spectral and spatial indices were equal, the best value of

α^i, for the ith band of the determined scene, will be obtained by the intersection point between the curves of spectral and spatial quality. Its value will depend exclusively on the characteristics of the source image (figure 2).

Additionally, to study the influence of the degradation level (n) of the MULTI image and the quantity of wavelet planes (W) to be integrated (equation (6)) in quality of the fused images, five information integration schemes, for the MULTI as well as the PAN image, have been evaluated at different degradation levels. The characteristics of each case and the results obtained are evaluated in the following section.

5. Results

The scenes used to investigate the different fusion schemes correspond to images captured on 12 February 2002 by panchromatic and multispectral sensors of the IKONOS satellite (Gonzalo and Lillo 2004), whose characteristics are summarized in table 1. The geographic location was the area of Maule Valley, Chile. Figure 3(*a*) and (*b*) represent the MULTI and PAN source images of the described area, respectively.

As noted in section 4, five particular schemes of the proposed fusion method have been investigated, analysing the influence of the degradation level of the source images in the image where the fusion process is performed for both spatial and spectral quality of the resulting image. To achieve this, a spatial resolution ratio of

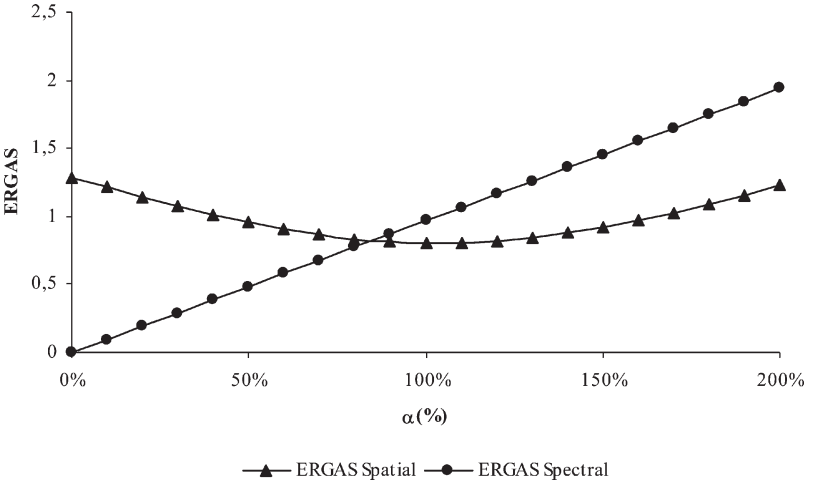

Figure 2. Determination of the value of α(%) for a spectral band.

Table 1. Spatial and spectral characteristics of the IKONOS sensor.

Band	Spectral resolution (nm)	Spatial resolution (m)
PAN	525.8–928.5	1
MS-1 (Blue)	444.7–516.0	4
MS-2 (Green)	506.4–595.0	4
MS-3 (Red)	631.9–697.7	4
MS-4 (NIR)	757.3–852.7	4

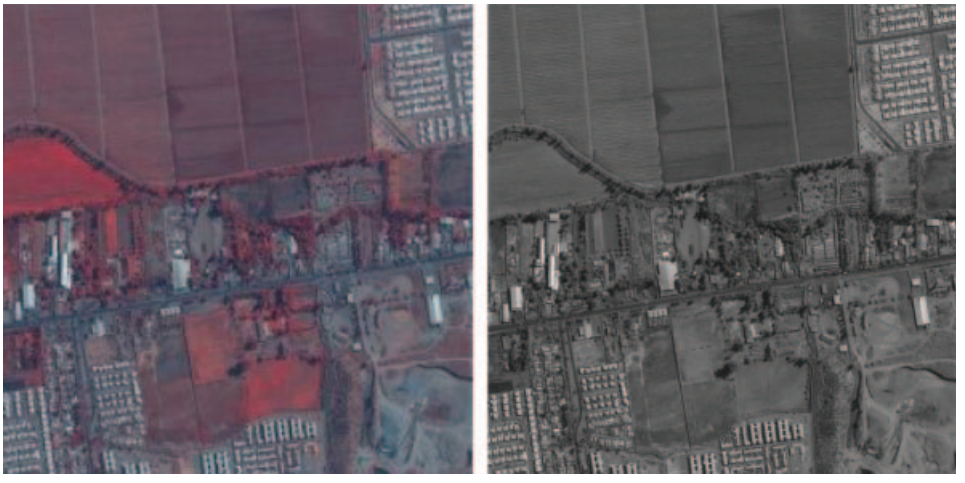

(*a*) (*b*)

Figure 3. False colour compositions (R=NIR, G=Green, B=Blue) of (*a*) the MULTI image and (*b*) the PAN image.

4 : 1 between the source images is considered, corresponding to the ratio between the spatial resolution of the multispectral (4 m) and panchromatic (1 m) sensors of the IKONOS satellite. This implies that the source images can be degraded in two levels ($n=1$ and $n=2$), and hence it is possible to obtain two sets of wavelet coefficients, one that contains the details between 1 m and 2 m and another that contains the details between 2 m and 4 m.

The spatial filter to obtain the first degradation level (h_j) is defined by equation (7) (Starck and Murtagh 1994):

$$h_j = \frac{1}{256}\begin{Bmatrix} 1 & 4 & 6 & 4 & 1 \\ 4 & 16 & 24 & 16 & 4 \\ 6 & 24 & 36 & 24 & 6 \\ 4 & 16 & 24 & 16 & 4 \\ 1 & 4 & 6 & 4 & 1 \end{Bmatrix} \tag{7}$$

To reach the second degradation level ($j+1$), it is necessary to apply the same spatial filter, but interlaying zeros between rows and columns (h_{j+1}), which is the motive of the name of the (*à trous*) algorithm (8):

$$h_{j+1} = \frac{1}{256}\begin{Bmatrix} 1 & 0 & 4 & 0 & 6 & 0 & 4 & 0 & 1 \\ 0 & 0 & 0 & 0 & 0 & 0 & 0 & 0 & 0 \\ 4 & 0 & 16 & 0 & 24 & 0 & 16 & 0 & 4 \\ 0 & 0 & 0 & 0 & 0 & 0 & 0 & 0 & 0 \\ 6 & 0 & 24 & 0 & 36 & 0 & 24 & 0 & 6 \\ 0 & 0 & 0 & 0 & 0 & 0 & 0 & 0 & 0 \\ 4 & 0 & 16 & 0 & 24 & 0 & 16 & 0 & 4 \\ 0 & 0 & 0 & 0 & 0 & 0 & 0 & 0 & 0 \\ 1 & 0 & 4 & 0 & 6 & 0 & 4 & 0 & 1 \end{Bmatrix} \tag{8}$$

Both filters are shown graphically in figure 4. The definition of the schemes follows a general nomenclature in which the acronym WA corresponds to the method name (wavelet *à trous* fusion method), and the letters M and P correspond to the MULTI and PAN images with their respective degradation levels. Figure 5 shows the general flowchart of the proposed method.

(i) WA_M_P12: The wavelet coefficients are integrated from the first degradation of the PAN image, which contains the spatial details between 1 m and 2 m, directly to the *i*th band of the MULTI.
(ii) WA_M_P1224: The wavelet coefficients are integrated from the first and second degradation of the PAN image, which contains the spatial details between 1 m and 2 m and between 2 m and 4 m, respectively, directly to the *i*th band of the MULTI.
(iii) WA_M12_P12: The wavelet coefficients are integrated from the first degradation of the PAN image, which contains the spatial details between 1 m and 2 m in the first degradation of the *i*th band of the MULTI image.
(iv) WA_M1224_P1224: The wavelet coefficients are integrated from the first and second degradation of the PAN image, which contain the spatial details between 1 m and 2 m and between 2 m and 4 m, respectively, in the second degradation of the *i*th band of the MULTI image.
(v) WA_M12_P1224: The wavelet coefficients are integrated from the first and second degradation of the PAN image, which contains the spatial details between 1 m and 2 m and between 2 m and 4 m, respectively, in the first degradation of the *i*th band of the MULTI image.

Table 2 presents the values of α^i corresponding to the points of the characteristic curves for the studied images for the four bands of the multispectral sensor of the IKONOS satellite and for the five researched schemes.

In order to study the spatial as well as the spectral quality provided by the five proposed configurations in this paper, based on the weighted wavelet *à trous* fusion method ($\alpha \neq 100\%$), the fused images were obtained using the values of α^i, described in section 4, and determined by the cutting point of the curves characteristic for each of the schemes.

The average spatial and spectral quality of the fused images was evaluated objectively by means of the ERGAS (spatial and spectral) indexes (equations (3)–(5)). These values along with their mean value and corresponding typical deviation are summarized in table 3, where additionally, in order to compare the results with

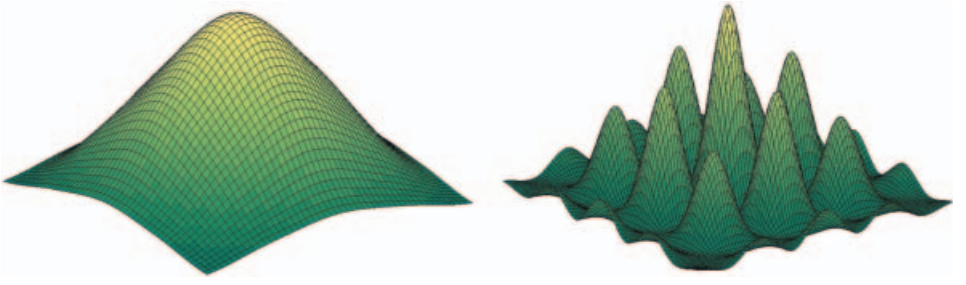

(*a*) (*b*)

Figure 4. Spatial filters: (*a*) h_j and (*b*) h_{j+1}.

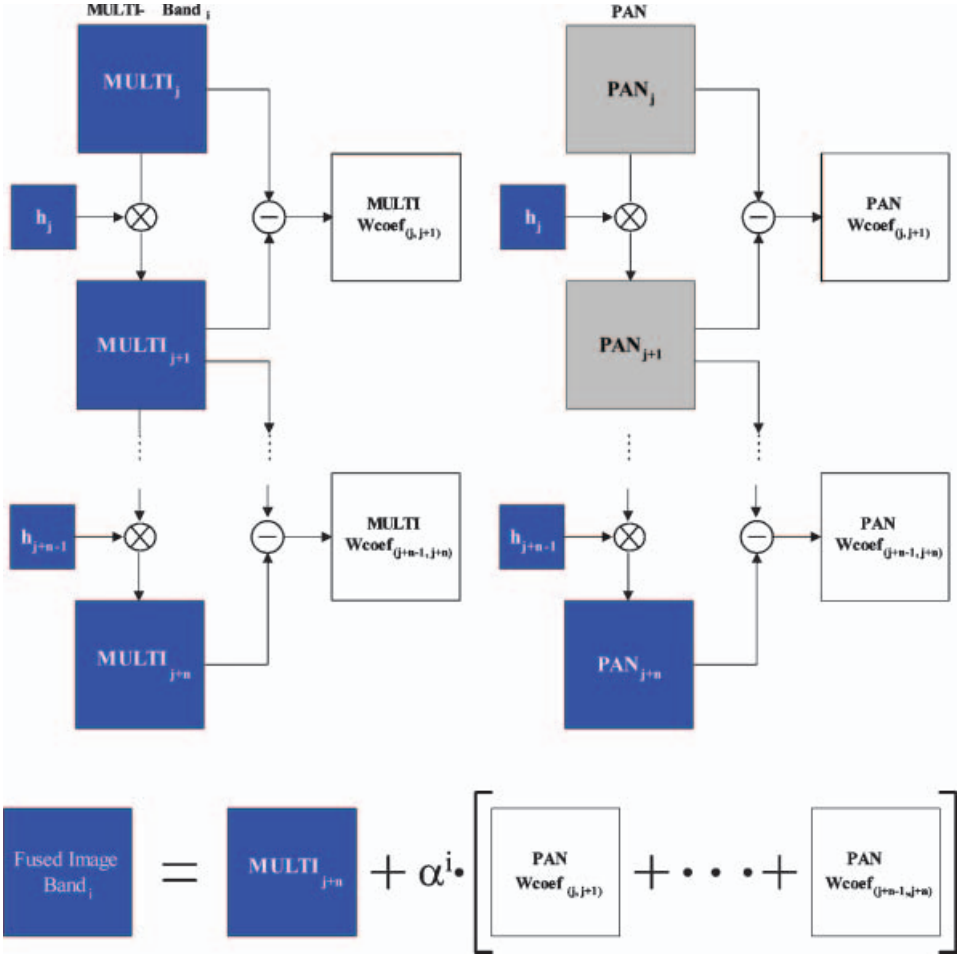

Figure 5. General flowchart of the proposed method.

other fusion methods, the same values have been represented by fused images through the standard *à trous* algorithm (α=100%), Mallat algorithm (Zhou *et al.* 1998, Zhang 1999) and filtering in Fourier domain (Ghassemian 2001, Lillo-Saavedra *et al.* 2005).

Analysing the results shown in table 3, it can be seen that the spatial quality of the fused images through the *à trous* algorithm, for both the standard and weighted

Table 2. Values of α^i(%) for the five cases analysed.

	Spectral band (%)			
Method	Blue	Green	Red	NIR
WA_M_P12	134.51	131.76	149.52	169.79
WA_M_P1224	84.91	85.39	99.33	113.15
WA_M12_P12	131.15	126.92	141.64	158.63
WA_MP12_P1224	82.35	81.48	93.03	104.30
WA_M1224_P1224	81.24	78.11	85.42	93.66

Table 3. Evaluation of spectral and spatial quality of the fused images.

Method		ERGAS			
		Spatial	Spectral	Average	St. Deviation
WA_M_P12	$\alpha \neq 100\%$	1.128	1.128	1.128	0.000
	$\alpha = 100\%$	1.279	0.770	1.025	0.360
WA_M_P1224	$\alpha \neq 100\%$	1.035	1.036	1.035	0.001
	$\alpha = 100\%$	1.025	1.079	1.052	0.038
WA_M12_P12	$\alpha \neq 100\%$	1.075	1.076	1.075	0.001
	$\alpha = 100\%$	1.094	0.772	0.933	0.228
WA_M12_P1224	$\alpha \neq 100\%$	0.976	0.977	0.977	0.001
	$\alpha = 100\%$	0.960	1.081	1.020	0.085
WA_M1224_P1224	$\alpha \neq 100\%$	0.914	0.915	0.914	0.001
	$\alpha = 100\%$	0.874	1.084	0.979	0.149
Wavelet Mallat		1.599	1.011	1.305	0.415
Fourier		1.491	1.231	1.361	0.184

cases, is superior to that of the images fused by the Mallat algorithm or by the filter in the Fourier domain. However, for all the cases studied, it is not the case that the spectral quality of the images fused by the *à trous* algorithm surpasses that of the images fused by Mallat. Thus, for $\alpha = 100\%$, the spectral quality is worse when the PAN image is degraded twice, while for $\alpha \neq 100\%$, the spectral quality increases with the degradation level. This can be justified on the basis of the spectral and spatial quality trade-off provided by the proposed method, which allows the reduction of the spectral information integrated in the fused image from the PAN image, without degrading its spatial quality. However, given that a trade-off between the spatial and spectral quality of the fused images is being sought, it should be noted that the strategies based on the *à trous* algorithm provide in all cases an inferior average value of the ERGAS indexes as well as notably reducing the standard deviation values. Indeed, for the case $\alpha \neq 100\%$ they are close to zero in the five cases studied. In this sense, it can be affirmed that the proposed method provides a better spectral–spatial quality trade-off for the fused images than the other three methods analysed, when the source images are degraded an appropriate number of levels.

The ERGAS values, both spatial and spectral, obtained for the five researched strategies show that even if for WA_M12_P12 with $\alpha = 100\%$, a better spectral quality is obtained and for the case WA_M_P1224 with $\alpha = 100\%$ the best spatial quality is obtained, the lowest average value with a low standard deviation is obtained by WA_M1224_P1224 with $\alpha \neq 100\%$. This result indicates that for all the analysed strategies, this one best establishes a spectral–spatial quality trade-off.

Figure 6 presents false colour compositions (R = Near-infrared, G = Green, B = Blue) of an original image zoom (figure 6(*a*)), and the corresponding zooms of fused images for the cases with the best spatial quality, WA_M_P1224 with $\alpha = 100\%$ (figure 6(*b*)), the best spectral quality, WA_M12_P12 with $\alpha = 100\%$ (figure 6(*c*)), and the best spatial–spectral quality trade-off, WA_M1224_P1224 with $\alpha \neq 100\%$ (figure 6(*d*)). In figure 6(*b*) (Zhang 2002), high spatial quality can be observed due to the information provided by the PAN image, but low spectral quality is evident in the high colour contrast. However, in figure 6(*c*), a low contrast is found, which prejudices its spatial quality while having a high spectral content. These two results

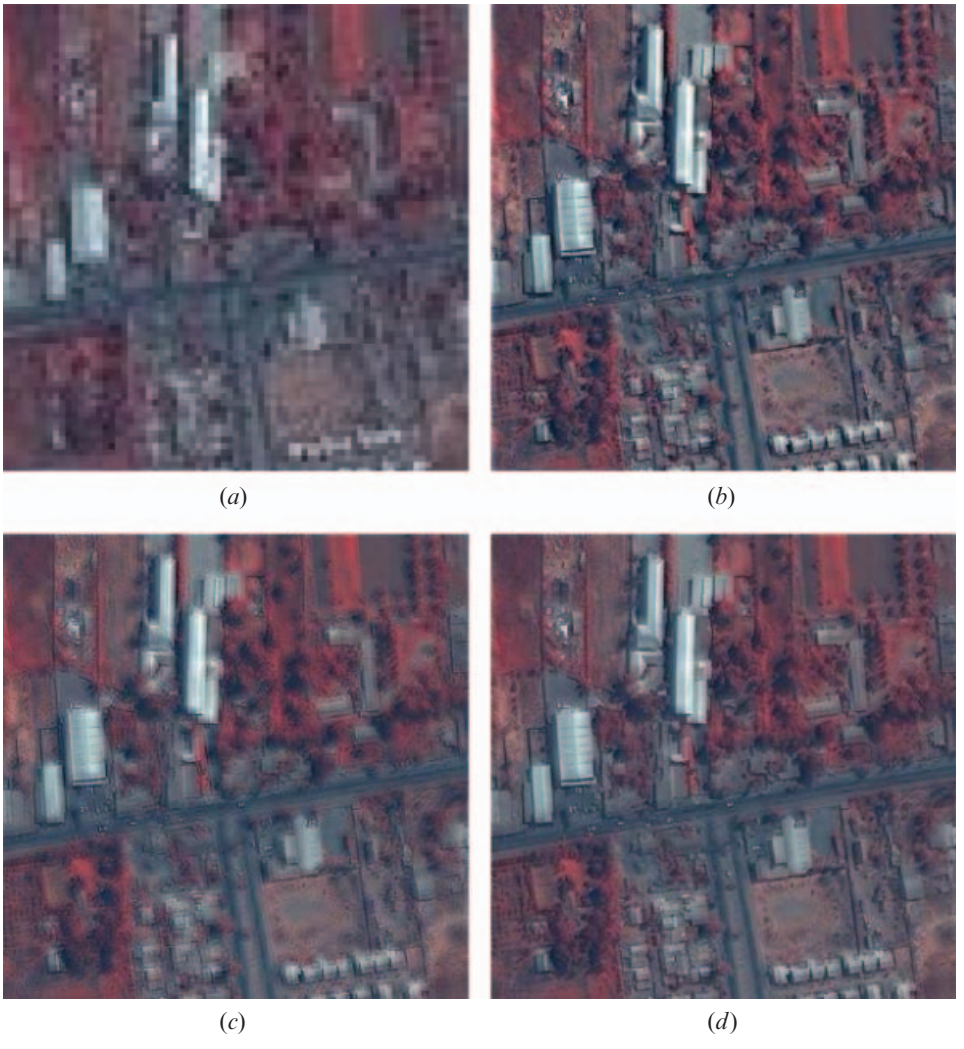

Figure 6. False colour compositions (R=NIR, G=Green, B=Blue). Zoom of original MULTI image (*a*), and zooms of the fused images: (b) WA_M_1224_P1224 with $\alpha=100\%$, (*c*) WA_M12_P12 with $\alpha=100\%$, (*d*) WA_M1224_P1224 with $\alpha\neq100\%$.

are opposite outputs from a fusion process without the spectral and spatial quality control of the fused images. Finally, in figure 6(*d*) the equilibrium between the spatial and spectral quality of the source images can be clearly appreciated.

6. Conclusions

This paper has proposed a methodology to determine the characteristic curves that permit the graphic estimation of the spatial and spectral quality trade-off of a fused image. To this end, this study proposes a new fusion criterion that weights, with a factor α, the coefficients of the PAN image to be fused through the wavelet *à trous* algorithm. The characteristics of the resulting image remain conditioned by the user's interest in having an image of very high spectral quality, very high spatial quality, or both qualities equilibrated.

This methodology has been used to determine the degradation level at which the fusion should be performed to minimize the noisy factors implicit in this process (resampling of the MULTI image). We concluded that the number of times that source images should be degraded should be equal to the relationship existing between the number of pixels of the PAN and MULTI images to obtain the best fusion results. In the case studied, an average ERGAS value of 0.914 was obtained, with a typical deviation between the spectral and spatial ERGAS of 0.001. The proposed methodology has improved the spatial–spectral quality of the fused images by the order of 30% with respect to the images fused by the Mallat and Fourier algorithms.

References

Candès, E.J. and Donoho, D.L., 2000, Curvelets, multiresolution representation, and scaling laws. In *Wavelet Applications in Signal and Image Processing VIII*, A. Aldroubi, A.F. Laine and M.A. Unser (Eds), Proceedings SPIE 4119, pp. 1–12.

Chibani, Y. and Houacine, A., 2002, The joint use of IHS transform and redundant wavelet decomposition for fusing multispectral and panchromatic images. *International Journal of Remote Sensing*, **23**, pp. 3821–3833.

Chibani, Y. and Houacine, A., 2003, Redundant versus orthogonal wavelet decomposition for multisensor image fusion. *Pattern Recognition*, **36**, pp. 879–887.

Dutilleux, P., 1987, An implementation of the algorithm *à trous* to compute the wavelet transform. In *Compt-rendus du congrès ondelettes et méthodes temps-fréquence et espace des phases*, J. Combes, A. Grossman and Ph. Tehanitchian (Eds), pp. 298–304 (Marseille: Springer-Verlag).

Garzelli, A., Nencini, F., Alparone, L., Aiazzi, B. and Baronti, S., 2004, PAN-sharpening of multispectral images: a critical review and comparison. *Geoscience and Remote Sensing Symposium, IGARSS '04. Proceedings. IEEE International*, **1**, pp. 81–84.

Ghassemian, H., 2001, Multi-sensor image fusion using multirate filter banks. *International Conference on Image Processing*, **1**, pp. 846–849.

González-Audicana, M., Otazu, X., Fors, O. and Seco, A., 2005. Comparison between the Mallat's and the *à trous* discrete wavelet transform based algorithms for the fusion of multispectral and panchromatic images. *International Journal of Remote Sensing*, **26**, pp. 597–616.

González-Audicana, M., Saleta, J., Catalán, O.G. and García, R., 2004, Fusion of multispectral and panchromatic images using improved IHS and PCA mergers based on wavelet decomposition. *IEEE Transactions on Geoscience and Remote Sensing*, **42**, pp. 1291–1299.

Gonzalo, C. and Lillo, M., 2004, Customized fusion of satellite images based on a new *à trous* algorithm. In *Image and Signal Processing for Remote Sensing X*, L. Bruzzone (Ed), Vol. 5573, pp. 444–451 (Bellingham, WA: SPIE).

Lillo-Saavedra, M., Gonzalo, C., Arquero, A. and Martinez, E., 2005, Fusion of multispectral and panchromatic satellite sensor imagery based on tailored filtering in the Fourier domain. *International Journal of Remote Sensing*, **26**, pp. 1263–1268.

Mallat, S., 1999, *A Wavelet Tour of Signal Processing*, 2nd edn (San Diego: Academic Press).

Núñez, J., Otazu, X., Fors, O., Prades, A., Palá, V. and Arbiol, R., 1999, Multiresolution-based image fusion with additive wavelet decomposition. *IEEE Transactions on Geoscience and Remote Sensing*, **37**, pp. 1204–1211.

Pohl, A., 1999, Tools and methods for fusion of images of different spatial resolution. In *International Archives of Photogrammetry and Remote Sensing*, E. Baltsavias, B.

Csatho, M. Hahn, B. Koch, A. Sieber, L. Wald and D. Wang (Eds), 3–4 June Valladolid, Spain, Vol. 32, Part 7-4-3 W6.

POHL, C. and VAN GENDEREN, J.L., 1998, Multisensor image fusion in remote sensing: concepts, methods and application. *International Journal of Remote Sensing*, **19**, pp. 823–854.

RANCHIN, T. and WALD, L., 2000, Fusion of high spatial and spectral resolution image: the ARSIS concept and its implementation. *Photogrammetric Engineering and Remote Sensing*, **66**, pp. 49–61.

STARCK, J.L. and MURTAGH, F., 1994, Image restoration with noise suppression using the wavelet transform. *Astronomy and Astrophysics*, **288**, pp. 342–350.

WALD, L., 2000, Quality of high resolution synthesized: is there a simple criterion? In *Proceedings of the International Conference on Fusion of Earth Data*, T. Ranchin and L. Wald (Eds), SEE/URISCA, France, pp. 99–105.

ZHANG, Y., 1999, A new merging method and it spectral and spatial effects. *International Journal of Remote Sensing*, **20**, pp. 2003–2014.

ZHANG, Y., 2002, Problems in the fusion of commercial high-resolution satellite images as well as Landsat 7 images and initial solution. *International Archives of Photogrammetry and Remote Sensing (IAPRS)*, **34**, Part 4.

ZHOU, J., CIVCO, D.L. and SILANDER, J.A., 1998, A wavelet method to merge Landsat TM and SPOT panchromatic data. *International Journal of Remote Sensing*, **19**, pp. 743–757.